
Development of Hybrid Systems: Interfacing a Silicon Neuron to a Leech Heart Interneuron

Mario F. Simoni¹, Gennady S. Cymbalyuk^{2,3}, Michael Q. Sorensen¹,
Ronald L. Calabrese², and Stephen P. DeWeerth¹

¹Laboratory for Neuroengineering
Georgia Institute of Technology
Atlanta, GA 30332-0363
{mario, sorensen, steve.deweerth}@ece.gatech.edu

²Department of Biology
Emory University
1510 Clifton Road
Atlanta, GA 30322
{gcym, rcalabre}@biology.emory.edu

³Institute of Mathematical Problems in Biology RAS
Pushchino, Moscow Region, Russia 142292 (on leave)

Abstract

We have developed a silicon neuron that is inspired by a mathematical model of the leech heartbeat (HN) interneuron. The temporal and ionic current behaviors of this silicon neuron are close to that of the living cell. Because of this similarity we were able to interface this silicon neuron to a living HN cell using a dynamic clamp technique [8]. We present data showing dynamic behaviors of the hybrid half-center oscillator.

1. Introduction

The development of hybrid systems, where living neurons are interfaced to electronic circuits, is a novel and promising tool to study the complex behaviors of neurosystems. Analog very large scale integrated (aVLSI) circuits have been used effectively to model the behavior of neurosystems in real-time. This technology was applied successfully to model individual neurons and small networks of neurons[3][9][10]. These silicon neurons provided insight into the dynamic behavior of the living neurons under real world conditions, complementing results obtained from mathematical modeling[6][1]. Thus, we believe that hybrid systems will provide further insight into mechanisms governing network behavior.

Our interest in hybrid systems is to develop a better understanding of motor pattern generation. The neural network controlling the leech heartbeat is based on two elemental oscillatory systems. Each consists of two reciprocally inhibitory HN neurons, which produce a half-center oscillator configuration. These neurons possess dynamics, such as escape and release properties, that are appropriate for alternating burst generation in this configura-

tion [11][12]. Furthermore, this oscillatory network and the HN neurons were extensively studied, and a detailed mathematical model employing Hodgkin-Huxley formalism was developed [5].

We are developing the technology to implement a variety of specific neuron models as aVLSI circuits. Here, we have designed and fabricated an aVLSI neuron circuit that was inspired by the mathematical model of the leech HN cell. In this paper we: 1) describe our silicon model of the leech HN cell and its behavior; 2) describe a hybrid half-center oscillator where the silicon HN cell is coupled with reciprocal inhibition to a living HN cell using a dynamic clamp technique[8]; and 3) describe the observed behavior of the hybrid system.

2. Silicon neuron

Our silicon neuron is inspired by a mathematical model of the leech HN cell that was mentioned previously[5]. This mathematical model consists of a leak conductance and eight voltage-gated conductances. To simplify the aVLSI circuits, however, we eliminated two of the voltage-gated conductances that are not crucial for producing the desired bursting behavior. The silicon neuron consists of seven modules, each with a current output that represents one of the seven ionic currents we are modeling: 1) a leak current I_{leak} , 2) a fast sodium current I_{Na} , 3) an inactivating potassium current I_{K1} , 4) a slowly activating and inactivating calcium current I_{CaS} , 5) a slowly activating and non-inactivating potassium current I_{K2} , 6) a persistent sodium current I_{P} , and 7) a hyperpolarization-activated inward current I_{h} . These seven currents are summed onto a capacitor, whose voltage represents the membrane potential of the cell. We model a particular ionic current by setting the parameters of a module that correspond to biophysical properties of neuronal ionic currents such as reversal potential, time constants for activation and inactivation, half-maximal values for activation and inactivation, and maximum conductance.

As shown in Figure 1A the output currents of the seven modules are summed onto capacitor C_{mem} to form the membrane potential V_{mem}

$$C_{\text{mem}} \frac{dV_{\text{mem}}}{dt} = I_{\text{leak}} + I_{\text{Na}} + I_{\text{P}} + I_{\text{K1}} + I_{\text{K2}} + I_{\text{CaS}} + I_{\text{h}} \quad (1)$$

Figure 1B is a circuit schematic of the building blocks we use to model the ionic currents. The formal derivation of the equations that describe the aVLSI circuits of the silicon neuron are found in [4]. Each of the voltage dependent currents consists of an output block and at least one of the state blocks depending on the dynamics of the current. The output current is described by the following equation where the subscript “ion” should be replaced by one of the particular ionic currents described previously

$$I_{\text{ion}} = \bar{g}_{\text{ion}} Z \tanh(S_{\text{ion}}(E_{\text{ion}} - V_{\text{mem}})) \text{ where } Z = \frac{m_{\text{ion}} h_{\text{ion}}}{I_{\tau_{\text{m_ion}}} I_{\tau_{\text{h_ion}}}} \quad (2)$$

where \bar{g}_{ion} represents the maximum ionic current, m_{ion} and h_{ion} are respectively the activation and inactivation states, $I_{\tau_{\text{m_ion}}}$ and $I_{\tau_{\text{h_ion}}}$ are normalization factors for m_{ion} and h_{ion} to be discussed later, $S_{\text{ion}} = \kappa/2U_{\text{T}}$ where $\kappa \approx 0.72$ is the gate efficiency of a MOSFET and $U_{\text{T}} = kT/q$ is the thermal voltage, and E_{ion} is the reversal potential of the current. The leak current uses only an output block and has a slightly different circuit from the other currents. Thus, for the leak current, $Z = 1$ and $S_{\text{leak}} = \kappa^2/(2U_{\text{T}}(1 + \kappa))$ in (2). In the case where a current uses only an activation or inactivation state then only the respective state with its normalization factor is used. The state_m and state_h blocks implement the activation and inactivation states, m_{ion} and h_{ion} , as the currents through transistors M6 and M9. The dynamics of the states are created by diode-capacitor integra-

tors consisting of transistor M6 and capacitor C_m for m_{ion} and transistor M9 and capacitor C_h for h_{ion} . The equations that describe the dynamics of these state variables are

$$\frac{dm_{ion}}{dt} = \tau_{m_{ion}} \left(\frac{m_{\infty_{ion}} - m_{ion}}{I_{\tau_{m_{ion}}}} \right), \text{ where } \tau_{m_{ion}} = \left(\frac{\kappa I_{\tau_{m_{ion}}}}{C U_T} \right) m_{ion} \text{ and} \quad (3)$$

$$m_{\infty_{ion}} = \frac{I_{\tau_{m_{ion}}}}{1 + \exp(A_{ion}(V_{m_{ion}} - V_{mem}))} \quad (4)$$

$$\frac{dh_{ion}}{dt} = \tau_{h_{ion}} \left(\frac{h_{\infty_{ion}} - h_{ion}}{I_{\tau_{h_{ion}}}} \right), \text{ where } \tau_{h_{ion}} = \left(\frac{\kappa I_{\tau_{h_{ion}}}}{C U_T} \right) h_{ion} \text{ and} \quad (5)$$

$$h_{\infty_{ion}} = \frac{I_{\tau_{h_{ion}}}}{1 + \exp(B_{ion}(V_{mem} - V_{h_{ion}}))} \quad (6)$$

$\tau_{m_{ion}}$ and $\tau_{h_{ion}}$ are the time constants for activation and inactivation, $m_{\infty_{ion}}$ and $h_{\infty_{ion}}$ represent the steady-state activation and inactivation functions. These functions are implemented as the output currents of source-degenerated differential pairs, which are sigmoidal functions of V_{mem} . It should be noted that $m_{\infty_{ion}}$ and $h_{\infty_{ion}}$ vary between 0 and $I_{\tau_{m_{ion}}}$ and $I_{\tau_{h_{ion}}}$ respectively, instead of 0 and 1, hence the need to normalize the states by these values in (2). $I_{\tau_{m_{ion}}}$ and $I_{\tau_{h_{ion}}}$ play two roles: 1) they control the time constants for activation and inactivation and 2) they are the maximum values of m_{ion} and h_{ion} . $A_{ion} = B_{ion} = (\kappa^2 / (U_T(1 + \kappa)))$ are inherent properties of the circuits. $V_{m_{ion}}$ and $V_{h_{ion}}$ are the membrane potentials at which $m_{\infty_{ion}}$ and $h_{\infty_{ion}}$ are at half their maximum value. The division by $I_{\tau_{m_{ion}}}$ in (3) and $I_{\tau_{h_{ion}}}$ in (5) result from factoring these terms to show how they affect the time constants. The output block uses an operational transconductance amplifier to scale the current I_{ion} by the maximum current \bar{g}_{ion} and account for

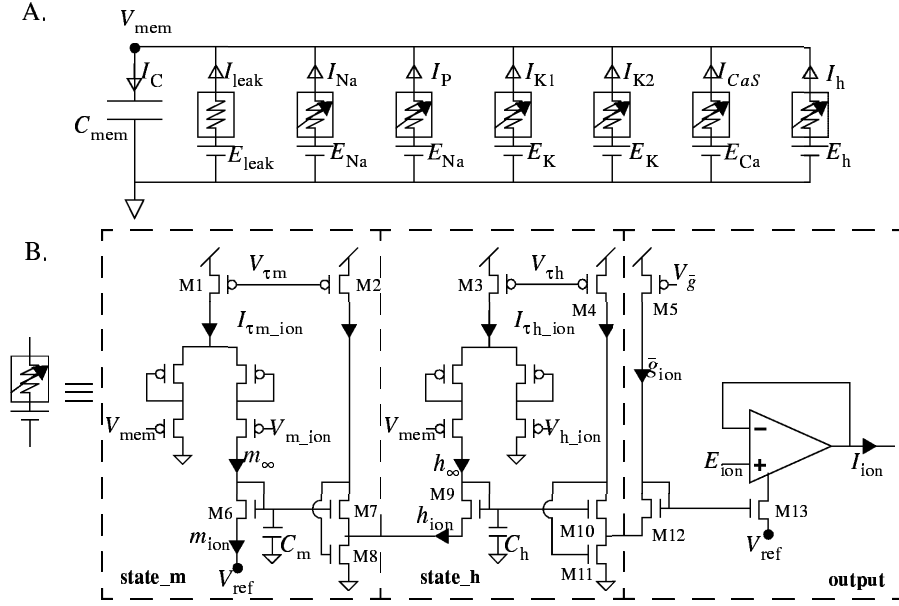


Figure 1: Schematic of the silicon neuron: A) the seven conductance modules whose currents sum on the membrane capacitor; open arrows indicate direction of positive current; B) the building blocks of the conductances.

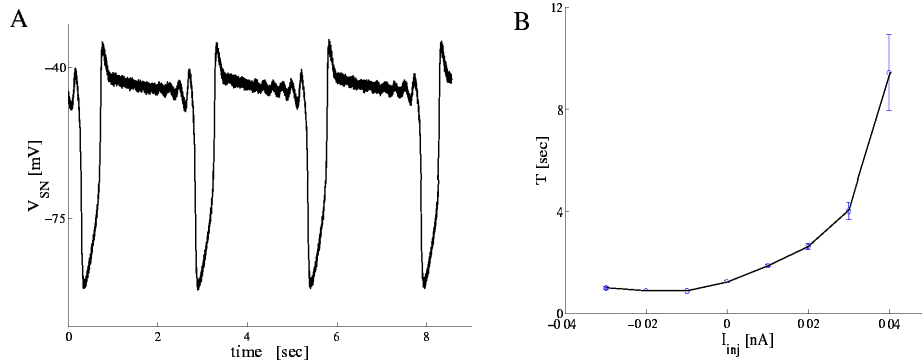


Figure 2: A) Membrane potential of the silicon neuron with parameters set for slow wave oscillations. B) Dependence of the period of the oscillations on injected current.

the effects of the reversal potential E_{ion} as shown in (2). The multiplication and division in (2) is performed by transistors M6 through M13 which form a translinear multiplier circuit. In the case where the current has only activation the drain of transistor M12 would be connected to transistors M7 and M8. For I_h we use only a state_h block to create a hyperpolarization activated current, in which case the source of M9 is connected to V_{ref} .

The parameters of the silicon neuron are controlled via a pair of digital-to-analog boards that we developed, called a PicStack[2]. The PicStack is connected by serial port to a computer, on which a Java applet creates a graphical user interface for setting the values of the D/A channels. This Java applet enables the user to control the parameters in real-time while the neuron is operating. Additionally, the applet provides the option to store parameters so that experiments can be repeated.

A subset of the ionic currents, which have slow dynamics, was shown to be important for producing the slow component of the bursting pattern in a half-center configuration [5][12]. Thus, as a starting point in testing the hybrid network, we used only I_h , I_{CaS} , I_{K2} , and I_p in the silicon neuron to create the slow waveform that is shown in Figure 2A. The leak current for the silicon neuron was implemented with the dynamic clamp where $E_{leak} = -100\text{mV}$ and $\bar{g}_{leak} = 30\text{nS}$. The dynamic clamp is an addition to standard electrophysiological equipment that provides real-time control over the injected current based on a user defined function and the measured membrane potential. Figure 2B illustrates the relationship between the period and the injected current. If the injected current becomes more negative than -0.03nA or more positive than 0.04nA the oscillations cease.

3. Hybrid system

The elemental leech heartbeat pattern generator consists of two HN cells interconnected through reciprocal inhibition. To make the hybrid system we replaced one of the HN cells with the silicon neuron. A single HN cell was isolated pharmacologically by application of bicuculline (1mM)[7]. We then used a dynamic clamp technique to introduce synaptic currents between the silicon and living neuron via separate electrometer units (Axoclamp2B, Axon Instruments) as shown in Figure 3. The membrane potential of the silicon neuron had to be scaled and shifted (we used typical operational amplifier circuits) to fit into the $\pm 200\text{mV}$ operating range of the dynamic clamp. However, effective currents for the silicon neuron are in the pA to nA range. Thus we connected the electrometer to the silicon neuron in a dual-electrode current-clamp mode with the voltage probe connected to the scale/shift output and the current electrode directly connected to C_{mem} of the circuit. The electrometer was connected to the living neuron in single-electrode discontinuous-current-

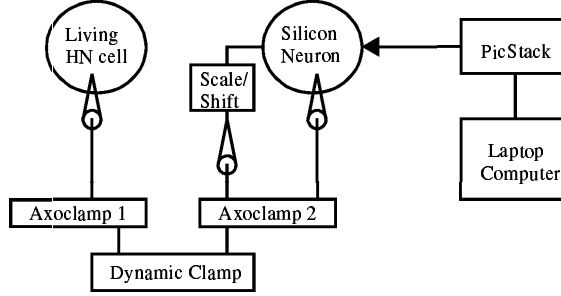


Figure 3: Schematic of the hybrid network.

clamp mode to measure the membrane potential and inject the synaptic current. Each of the synaptic currents were implemented by the dynamic clamp as

$$I_{\text{syn}} = \bar{g}_{\text{syn_post}} s (E_{\text{syn}} - V_{\text{mem}}) \quad \text{and} \quad \frac{ds}{dt} = \frac{1}{\tau_{\text{syn}} (1 - s_{\infty})} (s_{\infty} - s) \quad (7)$$

where $s_{\infty} = \tanh(G(V_{\text{pre}} - V_{\text{th_pre}}))$ for $V_{\text{pre}} > V_{\text{th}}$ and $s_{\infty} = 0$ for $V_{\text{pre}} < V_{\text{th}}$. $V_{\text{th_pre}}$ is the synaptic threshold voltage, E_{syn} is the synaptic reversal potential, s is the activation state of the current, V_{pre} is the presynaptic membrane potential, τ_{syn} is the time constant of activation, $\bar{g}_{\text{syn_post}}$ is the maximum synaptic conductance of the postsynaptic neuron. The subscripts “pre” and “post” are replaced by “SN” for the silicon neuron and “HN” for the living neuron. The multiplication of τ_{syn} by $(1 - s_{\infty})$ in (7) effectively creates two different time constants with a single dynamic equation.

The artificial leak conductance in the silicon neuron was adjusted so that it produced robust autonomous oscillations as shown in Figure 2A. The most important parameters for producing robust alternating oscillations in the hybrid network are the presynaptic threshold, V_{th} , and the postsynaptic maximal conductance, \bar{g}_{syn} , of the artificial synapses. These two parameters affect synaptic strength directly by determining both by the extent of threshold crossing by the presynaptic neuron and the maximal response of the postsynaptic neuron. In Figure 4A, oscillations began as soon as the dynamic clamp currents were implemented (arrow) and continued for several tens of cycles until the dynamic clamp was disabled. The period of the oscillation is longer than the free run period of the silicon neuron and the duty cycle of the two neurons is roughly equal; thus the system is producing true mutual oscillations. The thresholds were set so that the silicon neuron transmitted to the HN neuron throughout its depolarized plateau, but only the spikes of the HN neuron were transmitted to the silicon neuron. Thus in this configuration, transmission from the HN to the silicon neuron is spike mediated, but is graded from the silicon to the HN neuron. This configuration gave the most robust oscillation in three different preparations. Panels B-D are from a different preparation in which the thresholds of the synapses were varied. In B the threshold for the synapse from the HN neuron to the silicon neuron is too high for effective transmission and the autonomous oscillation of the silicon neuron drives the oscillations without feedback from the HN neuron. The duty cycle of the silicon neuron is longer than that of the HN neuron. In panel C the threshold for the synapse from the silicon neuron to the HN neuron was lowered by 5 mV. Inhibition is more robust leading to stronger hyperpolarization of the HN neuron and stronger rebound excitation. The tops of the spikes in the HN neuron now cross threshold and there is mild inhibitory feedback to the silicon neuron leading to a slightly prolonged period of the system compared to panel B. The duty cycle of the two neurons is nearly equal. In panel D the threshold for the synapse from the HN neuron to the silicon neuron was lowered. Now spike-mediated transmission (HN to SN) is robust (\bar{g}_{syn} had to be lowered slightly or oscillation ceased). The period of the system is greatly prolonged and the duty cycle of the HN neuron is pro-

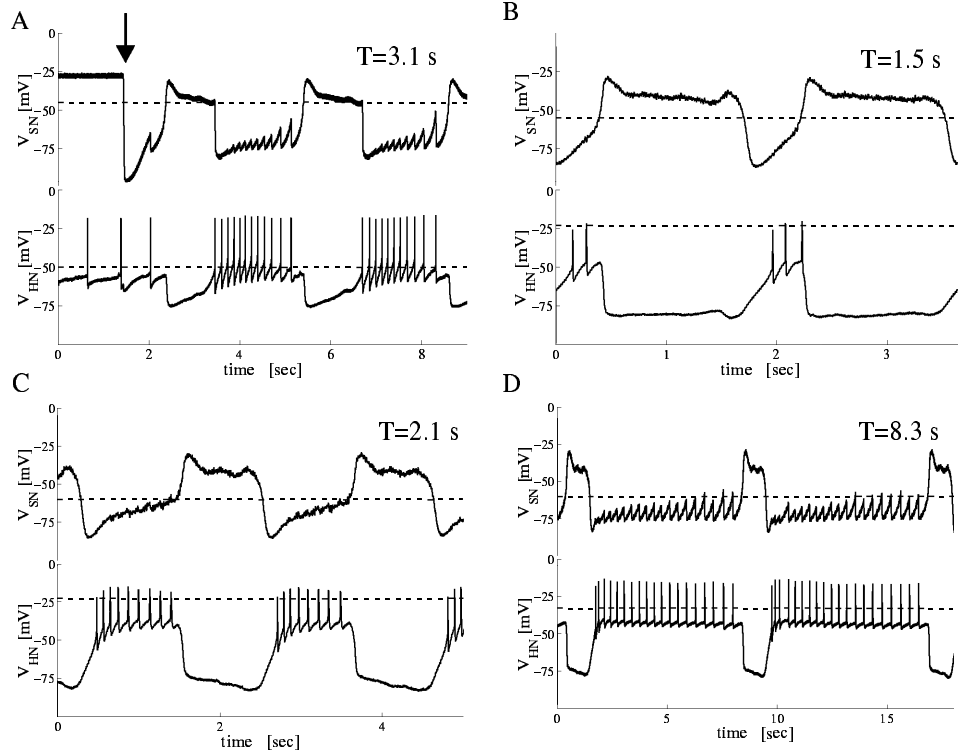


Figure 4: Plots of the membrane potentials of the silicon, V_{SN} , and living, V_{HN} , neurons for different values of V_{th} and \bar{g}_{syn} . The period, T , of the oscillations is denoted in the upper-right of each plot. The dashed lines denote V_{th} for the synapses. For A $\tau_{syn} = 0.1$ s and for B,C, and D $\tau_{syn} = 0.2$ s. The other synaptic parameters are
A) $\bar{g}_{syn_SN} = 200\text{nS}$, $\bar{g}_{syn_HN} = 50\text{nS}$, $V_{th_SN} = -45\text{mV}$, and $V_{th_HN} = -50\text{mV}$;
B) $\bar{g}_{syn_SN} = 500\text{nS}$, $\bar{g}_{syn_HN} = 10\text{nS}$, $V_{th_SN} = -55\text{mV}$, and $V_{th_HN} = -23\text{mV}$;
C) $\bar{g}_{syn_SN} = 500\text{nS}$, $\bar{g}_{syn_HN} = 10\text{nS}$, $V_{th_SN} = -60\text{mV}$, and $V_{th_HN} = -23\text{mV}$;
D) $\bar{g}_{syn_SN} = 400\text{nS}$, $\bar{g}_{syn_HN} = 10\text{nS}$, $V_{th_SN} = -60\text{mV}$, and $V_{th_HN} = -33\text{mV}$

longed with respect to the silicon neuron. Figure 4 indicates that the hybrid system's activity is a result of the interaction between the two neurons and is truly hybrid.

4. Discussion

We present here a novel hybrid system based on a silicon neuron and the neurons of the leech heartbeat pattern generation. Although our silicon neuron was designed to specifically model a leech HN cell, the parameters can be altered to obtain various different neuron properties. Moreover, because the circuit design is modular, the technology is in place to fabricate specific models of other types of neurons with minimal effort. The silicon neuron is portable and can be easily controlled via a computer. The voltage is easily scalable and the currents are in the proper range to interface directly with any standard electrophysiological equipment. With this hybrid system we were able to manipulate a living neuron to create a pattern generator with user-defined characteristics.

This work represents the first effort in our progression towards developing and studying hybrid systems of more complicated networks. In this paper we have demonstrated that a hybrid half-center oscillator can produce robust alternating oscillations, whose period and

duty cycle are determined by the intrinsic and synaptic properties of both the silicon and living neurons. These results encourage further exploration of hybrid systems as a tool for studying central pattern generators. We are progressively improving the silicon neuron design, including on chip synapses and scaling-amplifiers that will facilitate direct connections to the living neurons without the aid of a dynamic clamp. We are also developing electrode-embedded silicon substrates for culturing neurons so that we can make many extracellular connections to large networks of neurons. These particular steps will enable the construction and study of multiple cell hybrid networks that have been previously unapproachable.

Acknowledgments

MFS, MQS, and SPD were supported by NSF grant #IBN-9511721 and a Whitaker Foundation Biomedical Engineering Research Grant. RLC and GSC are supported by NIH grant NS24072. This work was inspired, in part, by collaborations at the NSF Sponsored Neuromorphic Engineering Workshop in Telluride, Colorado. Development of the Java applet was sponsored by a Sun Microsystems Academic Equipment Grant.

References

- [1]Cymbalyuk, G.S., Patel, G., Calabrese, R., DeWeerth, S.P., & Cohen, A. (2000) Modeling alternation to synchrony with inhibitory coupling: A neuromorphic VLSI Approach. *Neural Computation* 12 (in press).
- [2]Knight, C.D. (1999) WWW-Based Testing of Analog Circuits. Ph.D Thesis, Georgia Institute of Technology.
- [3]Le Masson, G., Le Masson, S., & Moulins, M. (1995) From Conductances to neural Network Properties: Analysis of Simple Circuits Using the Hybrid Network Method, *Prog. Biophys. molec. Biol.* 64(2): 201-220.
- [4]Mead, C.A. (1989) *Analog VLSI and Neural Systems*. Addison-Wesley, Reading, Ma.
- [5]Nadim, F., Olsen, O.H., De Schutter, E., & Calabrese, R.L. (1995) Modeling the leech heartbeat elemental oscillator. I. Interactions of intrinsic and synaptic currents. *Journal of Computational Neuroscience* 2(3):215-235.
- [6]Patel, G., Cymbalyuk, G.S., Calabrese, R.L., & DeWeerth, S.P. (1999) Bifurcation Analysis of a Silicon Neuron. In S. A. Solla, T. K. Leen, and K.-R. Mueller (eds.), *Advances in Neural Information Processing Systems 12*. Cambridge, MA: MIT Press.
- [7]Schmidt, J., & Calabrese, R.L. (1992) Evidence that acetylcholine is an inhibitory transmitter of heart interneurons in the leech. *Journal of Experimental Biology* 171:329-47.
- [8]Sharp, A.A., Skinner, F.K., & Marder, E. (1996) Mechanisms of oscillation in dynamic clamp constructed two-cell half-center circuits. *Journal of Neurophysiology* 76 (2):867-883.
- [9]Simoni, M.F., Patel, G.N., DeWeerth, S.P., & Calabrese, R.L. (1997) Analog VLSI Model of the Leech Heartbeat Elemental Oscillator. Sixth Annual Computational Neuroscience Meeting. NIH, NSF: Big Sky, Montana.
- [10]Simoni, M.F., & DeWeerth, S.P. (1999) Adaptation in an aVLSI Model of a Neuron. *IEEE Transactions on Circuits and Systems-II: Analog and Digital Signal Processing* 46(7):967-970.
- [11]Skinner, F.K., Kopell, N., & Marder, E. (1994) Mechanisms for oscillation and frequency control in reciprocally inhibitory model neural networks. *Journal of Computational Neurosciences* 1:69-87.
- [12]Wang, X.J., & Rinzler, J. (1992) Alternating and synchronous rhythms in reciprocally inhibitory model neurons. *Neural Computation* 4:84-87.